Locally Varying Anisotropy-Based Linearized Post-Stack Inversion

Anton Bogrash, Mauricio Sacchi, Jeff Boisvert

Spatial inverse problems aim to characterize spatially distributed phenomena being a subclass of more general inverse problems. Fundamentally, any inference from an indirect measurement could be posed as an inverse problem. Modern inverse modeling within the Earth science context has been mostly developed in geophysical community with gradually growing involvement of relevant adjacent disciplines. The current work is concerned with joint application of geostatistics and regularized seismic inversion. Vast majority of inverse problems are ill-posed with some of the most important difficulties being non-linearity, instability and non-uniqueness. While non-linear probabilistic inversion presents the research frontier, it is outside the scope of the current work. Linearized solution is adopted in the presented methodology and Tikhonov regularization is imposed as a constraint to address the latter two issues. Such mathematical simplicity and tractability come at a price of oversimplification of complex physical processes and their geological manifestation. Nevertheless, this presentation is intended to demonstrate that quantification of spatial continuity from geostatistical methods can significantly improve even a fairly basic linearized Gaussian inversion for acoustic impedance. Covariance matrices in the inversion estimates are the key components of a realistic solution. Reliable spatial covariance inference requires redundant measurements in all directions. However, a typical petroleum exploration issue is the lack of sufficient data points for robust horizontal covariance estimation. The main proposed idea is to use locally varying anisotropy (LVA) field estimated from seismic data to calculate the covariance matrix. The orientations could be derived directly from seismic which would also address nonstationarity. The proposed methodology is compatible with the state-of-the-art geostatistical, geophysical and geological modeling components of the reservoir characterization workflow at the exploration and appraisal stages.

Introduction

Inverse problems in geophysics count a few decades of history prompting rigorous mathematical treatment. Three major schools of thought emerged historically in Russia (Tikhonov, 1943, 1963), in USA (Backus & Gilbert, 1967, 1970) and in France (Tarantola, 2004; Tarantola & Valette, 1982).

The scope of this presentation is limited to seismic inversion constrained by the information on spatial continuity from geostatistical analysis. Note it is not the technique known by practitioners as geostatistical inversion (Deutsch, 2001) which also involves sequential simulation to generate realizations. Within petroleum industry context, inversion plays an important role in the reservoir characterization linking quantitative interpretation of the seismic data and well logs with the target properties of interest such as porosity, permeability, fluid saturation etc.

Problem formulation

Main issues with inverse problems are non-linearity, instability and non-uniqueness of solution. We only consider linearized solutions in the work presented here. For some of the latest developments on non-linear inversion we refer to, e.g. (Liu et al., 2018).

Seismic data contains much information on the geological structures than conventional geostatistical and geophysical methods use. Local anisotropy incorporated in geophysical inversion has been done by some researchers (Bongajum, Boisvert, & Sacchi, 2013; Pereira, Calçôa, Azevedo, Nunes, & Soares, 2020). The current work capitalizes on achievements of the former with main differences being extraction of the orientations directly from seismic data rather than from the true model of acoustic impedance and calculation of the varying magnitudes in the LVA field.

In geophysical context, linearized forward problem is typically expressed as

$$\mathbf{d} = G\mathbf{m} \tag{1}$$

where

$\mathbf{d}$ is the measured observations dataset,
$\mathbf{X}$ is the set of model parameters,
G is a forward operator representing a theory which predicts $\mathbf{d}$ from $\mathbf{m}$.

Specifically, in this project, $\mathbf{d} \equiv \mathbf{s}$ — the seismic record, $\mathbf{m} \equiv \mathbf{L_P}$ — logarithmic impedance and G — geophysical transform matrix, resulting in a convolutional model of a seismic trace without noise:

$$\mathbf{s} = G\mathbf{L_P} \tag{2}$$

Therefore, the cost function in least-squares sense with $\hat{\mathbf{L}}_\mathbf{P}$ being the estimate of $\mathbf{L_P}$ and assuming G can be constructed from a known wavelet w and a differential operator D (Madsen, Hansen, & Omre, 2020) could be written as

$$J(L_P) = \|\mathbf{s} - G\hat{\mathbf{L}}_\mathbf{P}\|_2^2 \tag{3}$$

Formulations with explicit performance metrics for image quality assessment acoustic property models, such as structural similarity index (SSIM) (Li et al., 2020) have been considered but simple root mean square error (RMSE) suits the current project better.

RMSE has been chosen as a loss function as it is fairly straightforward and suitable for the task:

$$RMSE = \sqrt{\frac{1}{N}\Sigma_{i=1}^{N}\left(\mathbf{r} - \hat{\mathbf{r}}\right)^2} \tag{4}$$

Pearson correlation coefficient has been selected as a measure of success:

$$PCC = \frac{\sum_{i=1}^{n}(x_i - \bar{x})(y_i - \bar{y})}{\sqrt{\sum_{i=1}^{n}(x_i - \bar{x})^2}\sqrt{\sum_{i=1}^{n}(y_i - \bar{y})^2}}, \tag{5}$$

where $\bar{x}$ and $\bar{y}$ are the averages for x and y, respectively.

Regularized inversion. A deterministic formulation of the linear inverse problem without is presented in (Scheidt, Li, & Caers, 2018, p. 168) citing (Tikhonov & Arsenin, 1977):

$$J(\mathbf{m}) = \|G\mathbf{m} - \mathbf{d}_{obs}\|_2^2 + \mu\|\mathbf{m} - \mathbf{m}_0\|_2^2, \tag{6}$$

where $\mathbf{m}_0$ is a reference model.

The solution to the objective function 6 is:

$$\hat{\mathbf{m}} = (G^T G + \mu I)^{-1}(G^T\mathbf{d}_{obs} + \mu\mathbf{m}_0) \tag{7}$$

Next, a formulation with weighting matrices is given:

$$J(\mathbf{m}) = \|W_d^T(G\mathbf{m} - \mathbf{d}_{obs})\|_2^2 + \mu\|W_m^T(\mathbf{m} - \mathbf{m}_0)\|_2^2 \tag{8}$$

Let us substitute the weighting matrices W_d and W_m with inverse of covariance Σ_d^{-1} and Σ_m^{-1}:

$$J(\mathbf{m}) = \|\Sigma_d^{-1/2}(G\mathbf{m} - \mathbf{d}_{obs})\|_2^2 + \mu\|\Sigma_m^{-1/2}(\mathbf{m} - \mathbf{m}_0)\|_2^2 \tag{9}$$

Denote the factorization of data covariance (assumed a diagonal matrix, i.e. uncorrelated noise):

$$\Sigma_d^{-1} = Q_d Q_d^T; [n \times m][m \times n] = [n \times n], \tag{10}$$

and similarly the model covariance:

$$\Sigma_m^{-1} = Q_m^T Q_m; [m \times n][n \times m] = [m \times m] \tag{11}$$

now expression 9 becomes:

$$J(\mathbf{m}) = \|Q_d Q_d^T (G\mathbf{m} - \mathbf{d}_{obs})\|_2^2 + \mu \|Q_m^T Q_m (\mathbf{m} - \mathbf{m}_0)\|_2^2 \tag{12}$$

Take the partial derivatives and equate to zero:

$$\frac{\partial J}{\partial \mathbf{m}^T} = 2G^T Q_d Q_d^T G\mathbf{m} - 2G^T Q_d Q_d^T \mathbf{d}_{obs} + 2\mu Q_m^T Q_m \mathbf{m} - 2\mu Q_m^T Q_m \mathbf{m}_0 = 0 \tag{13}$$

$$\mathbf{m}(G^T Q_d Q_d^T G + \mu Q_m^T Q_m) = G^T Q_d Q_d^T \mathbf{d}_{obs} + \mu Q_m^T Q_m \mathbf{m}_0 \tag{14}$$

$$\hat{\mathbf{m}} = (G^T Q_d Q_d^T G + \mu Q_m^T Q_m)^{-1} (G^T Q_d Q_d^T \mathbf{d}_{obs} + \mu Q_m^T Q_m \mathbf{m}_0) \tag{15}$$

The estimate above is equivalent to equation 6.55 in (Scheidt et al., 2018, p. 168). Next, let us take equation 9 assuming $\mathbf{m}_0 = 0$ and the regularization term $\mu = 1$:

$$J(\mathbf{m}) = \|\Sigma_d^{-1}(G\mathbf{m} - \mathbf{d}_{obs})\|_2^2 + \|\Sigma_m^{-1}(\mathbf{m})\|_2^2 \tag{16}$$

$$\frac{\partial J}{\partial \mathbf{m}^T} = 2G^T \Sigma_d^{-1} G\mathbf{m} - 2G^T \Sigma_d^{-1} \mathbf{d}_{obs} + 2\Sigma_m^{-1} \mathbf{m} = 0 \tag{17}$$

$$\mathbf{m}(G^T \Sigma_d^{-1} G + \Sigma_m^{-1}) = G^T \Sigma_d^{-1} \mathbf{d}_{obs} \tag{18}$$

$$\hat{\mathbf{m}} = (G^T \Sigma_d^{-1} G + \Sigma_m^{-1})^{-1} (G^T \Sigma_d^{-1}) \mathbf{d}_{obs} \tag{19}$$

Model setup

For the purposes of the current project, SEAM Phase I data has been generated from a simple geological model (Figure 1). The clastic subsection in the red dashed box consists of 125 traces with 40 m separation. Random Gaussian noise with signal-to-noise ratio has been added to the data.

LVA fields were estimated with *imorient* CCG program (Martin & Boisvert, 2017) and shown on Fig. 2. Noisier seismic data generally requires larger window size.

Results

Relative inversion. Conventional constant anisotropy covariance is more susceptible to variogram modeling errors as seen from the vertical striping artefacts in solution c) (Fig. 4). The overall relative inversion lacks a trend while reproducing the major dipping events.

Upon looking at the trace 55, it could be seen that constant geometric anisotropy inversion reproduces the trace shape better than LVA(too many additional impedance variations not existing in the original impedance)

and regularized solution — less pronounced layer detection.

Absolute inversion. Fig. 6 shows how inclusion of the LFM allows to achieve significant improvement in the estimation of absolute acoustic impedance values. Due to the low frequency component L_P 0 being so close to the true values in the current model setup, the regularized inversion slightly outperforms LVA-based one.

Table 1: Performance comparison between inversion methods.

Inversion method	$PCC\ I_P$	$RMSE\ I_P$	$PCC\ d_{tx}$	$RMSE\ d_{tx}$
Regularization	96.453	0.973	0.003	0.913
CGA-based	689.990	0.480	0.002	0.965
LVA-based	107.030	0.957	0.003	0.935

Conclusions and future work

Including spatial information shows an advantage over purely mathematical regularized least squares relative inversion. Missing low frequencies are critical for the absolute impedance values estimation: they could be derived from the available migration velocity cube or well logs. The shortcoming of current numerical experiment setup is that the difference between the LFM and true acoustic impedance values is fairly small. In a real world reservoir characterization project this would not be the case and one of the intended next steps is to build a low frequency model based on interpreted horizons so the kriging interpolation is bound to stratigraphic intervals.

In petroleum exploration context, practical difficulty of horizontal variogram inference presents a challenge. Although there are techniques developed to improve horizontal variogram reliability from the seismic (Rezvandehy & Deutsch, 2018), the variogram in Euclidean q-dimensional space (Boisvert & Deutsch, 2011) and respective inver of covariance matrix seems to be more stable in the inversion applications.

Another potentially fruitful research direction is stochastic Bayesian inversion where geostatistics brings value through complex geological priors quantification (Hansen, Cordua, & Mosegaard, 2012) and modeling multivariate relationship between the variables of different nature at different scales (Hadavand Siri & Deutsch, 2018).

More complex geological models are going to be investigated to determine the advantages of using the covariance matrix estimation with LVA with possible extension to pre-stack inversion.

References

Backus, G. E., & Gilbert, J. F. (1967, jul). Numerical Applications of a Formalism for Geophysical Inverse Problems. *Geophysical Journal International*, *13*(1-3), 247–276. Retrieved from `https://academic.oup.com/gji/article-lookup/doi/10.1111/j.1365-246X.1967.tb02159.x` doi: 10.1111/j.1365-246X.1967.tb02159.x

Backus, G. E., & Gilbert, J. F. (1970, mar). Uniqueness in the inversion of inaccurate gross Earth data. *Philosophical Transactions of the Royal Society of London. Series A, Mathematical and Physical Sciences*, *266*(1173), 123–192. doi: 10.1098/rsta.1970.0005

Boisvert, J. B., & Deutsch, C. V. (2011, apr). Programs for kriging and sequential Gaussian simulation with locally varying anisotropy using non-Euclidean distances. *Computers and Geosciences*, *37*(4), 495–510. doi: 10.1016/j.cageo.2010.03.021

Bongajum, E. L., Boisvert, J., & Sacchi, M. D. (2013). Bayesian linearized seismic inversion with locally varying spatial anisotropy. *Journal of Applied Geophysics*, *88*, 31–41. doi: 10.1016/j.jappgeo.2012.10.001

Deutsch, C. V. (2001). *A Short Note on: Stochastic Inversion for Integration of Seismic Data in Geostatistical Reservoir Modeling* (Tech. Rep.).

Hadavand Siri, M., & Deutsch, C. V. (2018). Multivariate stochastic seismic inversion with adaptive sampling. Retrieved from `http://library.seg.org/` doi: 10.1190/GEO2017-0025.1

Hansen, T. M., Cordua, K. S., & Mosegaard, K. (2012). Inverse problems with non-trivial priors: efficient solution through sequential Gibbs sampling. *Comput Geosci*, *16*, 593–611. doi: 10.1007/s10596-011-9271-1

Li, S., Liu, B., Ren, Y., Chen, Y., Yang, S., Wang, Y., & Jiang, P. (2020, mar). Deep-Learning Inversion of Seismic Data. *IEEE Transactions on Geoscience and Remote Sensing*, *58*(3), 2135–2149. doi: 10.1109/TGRS.2019.2953473

Liu, X., Li, J., Chen, X., Guo, K., Li, C., Zhou, L., & Cheng, J. (2018). Stochastic inversion of facies and reservoir properties based on multi-point geostatistics. Retrieved from https://doi.org/10.1088/1742-2140/aac694 doi: 10.1088/1742-2140/aac694

Madsen, R. B., Hansen, T. M., & Omre, H. (2020, feb). Estimation of a non-stationary prior covariance from seismic data. *Geophysical Prospecting*, *68*(2), 393–410. Retrieved from https://onlinelibrary.wiley.com/doi/abs/10.1111/1365-2478.12848 doi: 10.1111/1365-2478.12848

Martin, R., & Boisvert, J. B. (2017, dec). Iterative refinement of implicit boundary models for improved geological feature reproduction. *Computers and Geosciences*, *109*, 1–15. doi: 10.1016/j.cageo.2017.07.003

Pereira, P., Calçôa, I., Azevedo, L., Nunes, R., & Soares, A. (2020, may). Iterative geostatistical seismic inversion incorporating local anisotropies. *Computational Geosciences*, 1–16. Retrieved from https://link.springer.com/article/10.1007/s10596-020-09966-1 doi: 10.1007/s10596-020-09966-1

Rezvandehy, M., & Deutsch, C. V. (2018, may). Horizontal variogram inference in the presence of widely spaced well data. *Petroleum Geoscience*, *24*(2), 219–235. Retrieved from https://pg.lyellcollection.org/content/24/2/219https://pg.lyellcollection.org/content/24/2/219.abstract doi: 10.1144/petgeo2016-161

Scheidt, C., Li, L., & Caers, J. (2018). *Quantifying Uncertainty in Subsurface Systems*. Hoboken, NJ, USA: John Wiley & Sons, Inc. Retrieved from http://doi.wiley.com/10.1002/9781119325888 doi: 10.1002/9781119325888

Tarantola, A. (2004). *Inverse Problem Theory and Methods for Model Parameter Estimation*. Society for Industrial and Applied Mathematics. doi: 10.1137/1.9780898717921

Tarantola, A., & Valette, B. (1982). *Inverse Problems = Quest for Information* (Vol. 50; Tech. Rep.).

Tikhonov, A. N. (1943). On the stability of inverse problems. *Doklady Akademii Nauk SSSR*, *39*(5), 195–198.

Tikhonov, A. N. (1963). Solution of incorrectly formulated problems and the regularization method. *Doklady Akademii Nauk SSSR*, *151*, 501–504. Retrieved from http://www.mathnet.ru/rus/agreement

Tikhonov, A. N., & Arsenin, V. I. A. (1977). Solutions of ill-posed problems. , xiii, 258 p. :.

Figures

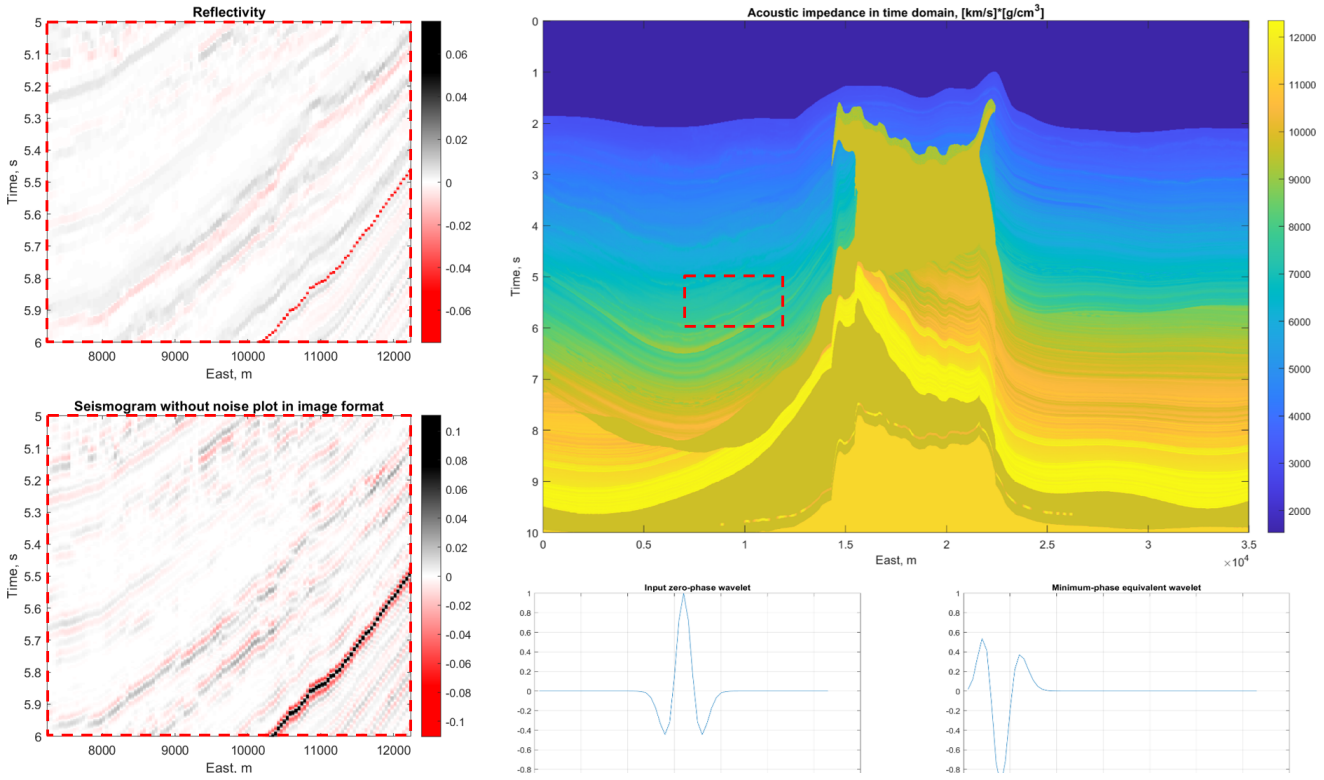

Figure 1: SEAM Phase I acoustic impedance converted to time domain. A small clstic section in the dashed box has been used for subsequent numercal experiments. Seismic record is generated fro reflectivity convolved with a minimum phase 25 Hz Ricker wavelet.

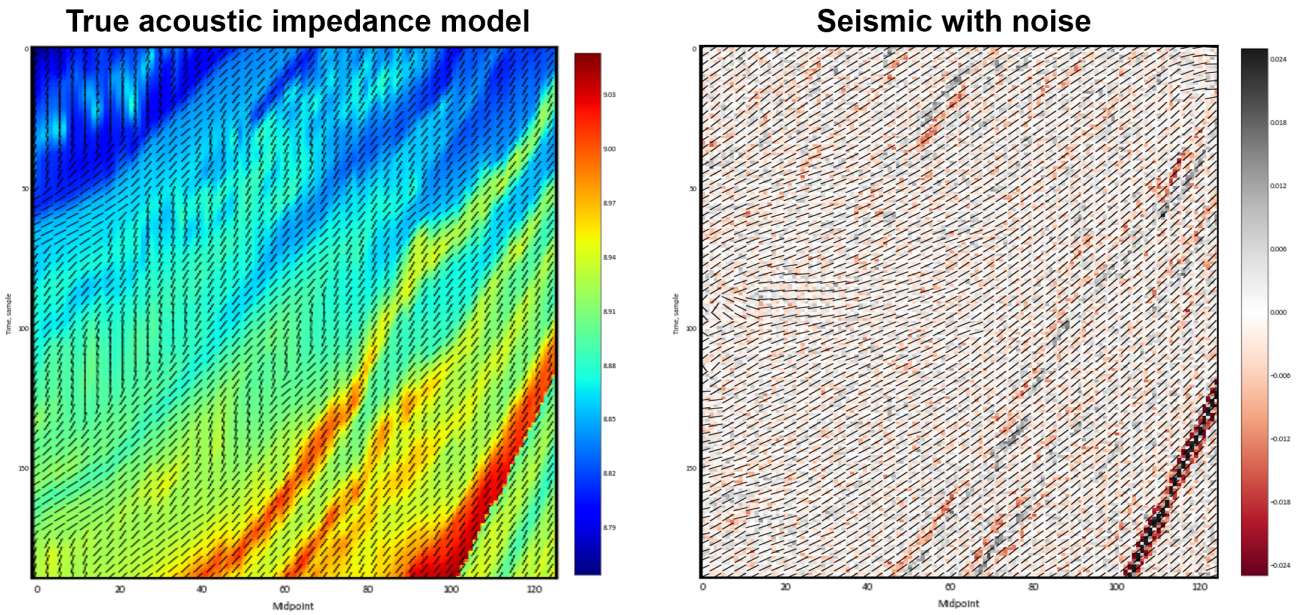

Figure 2: LVA orientation fields from the true P-impedance (left) and seismic data (right) are shown. The LVA field from seismic is used for subsequent inversion estimates.

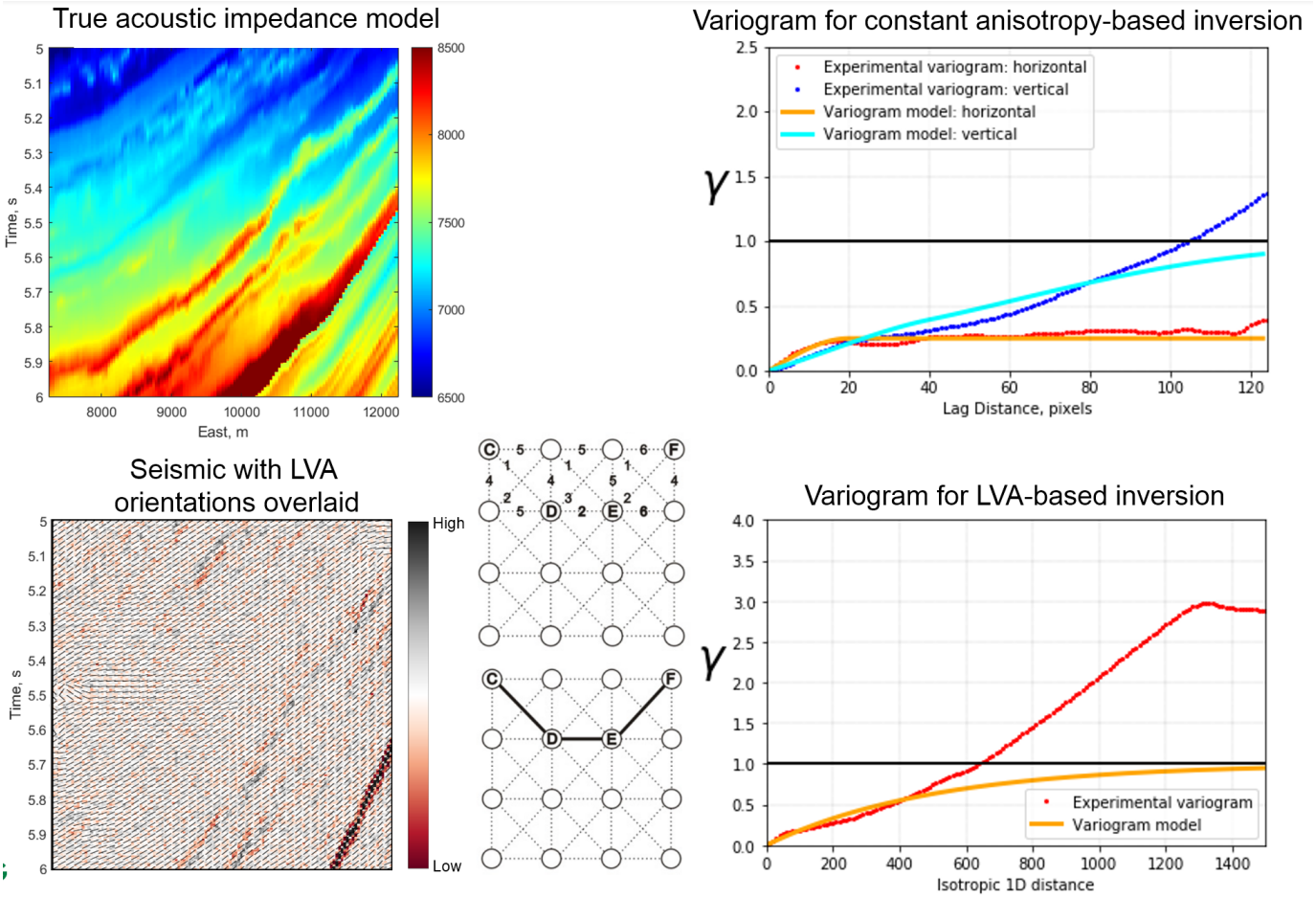

Figure 3: Covariance estimation from the true P-impedance model. Constant geometric anisotropy relies on Euclidean distances only whereas LVA covariance takes the shortest path distance and isotropic variogram in q dimensions after multidimensional scaling (Boisvert & Deutsch, 2011) is shown.

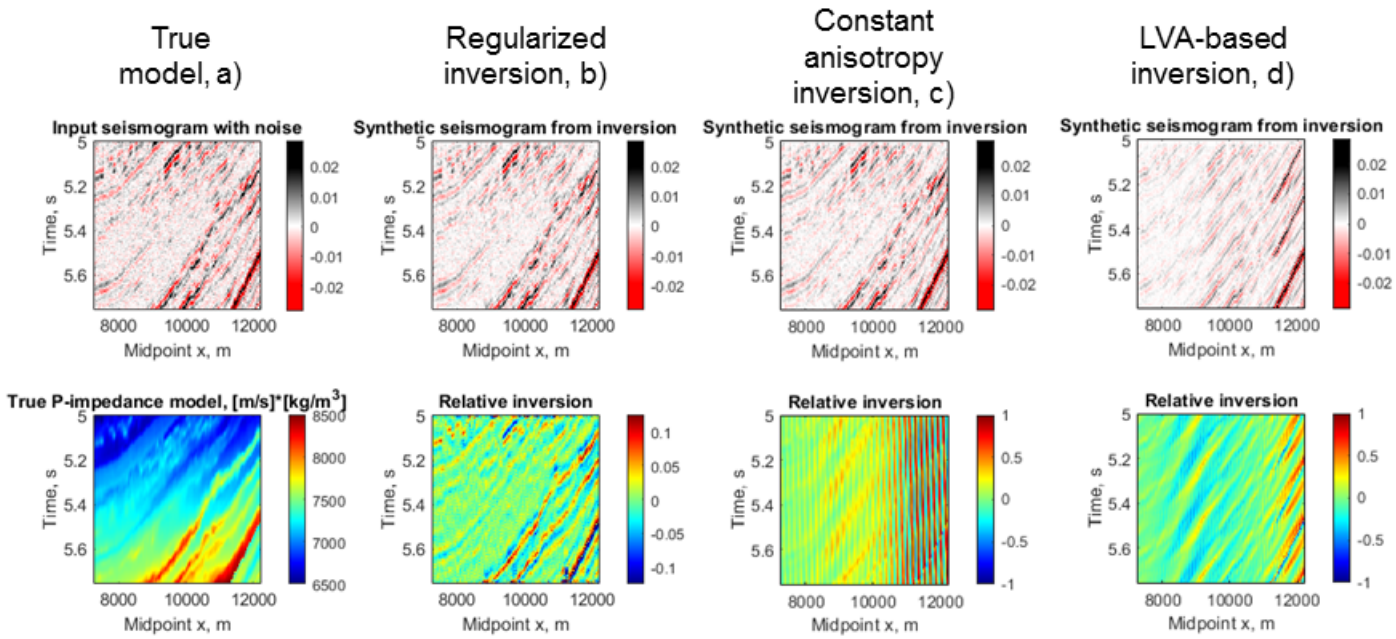

Figure 4: Comparison between relative inversion configurations. Top row represents seismograms whereas the bottom is P-impedance: a) True model; b) regularized inversion; c) constant geometric anisotropy-based inversion; d) LVA-based inversion.

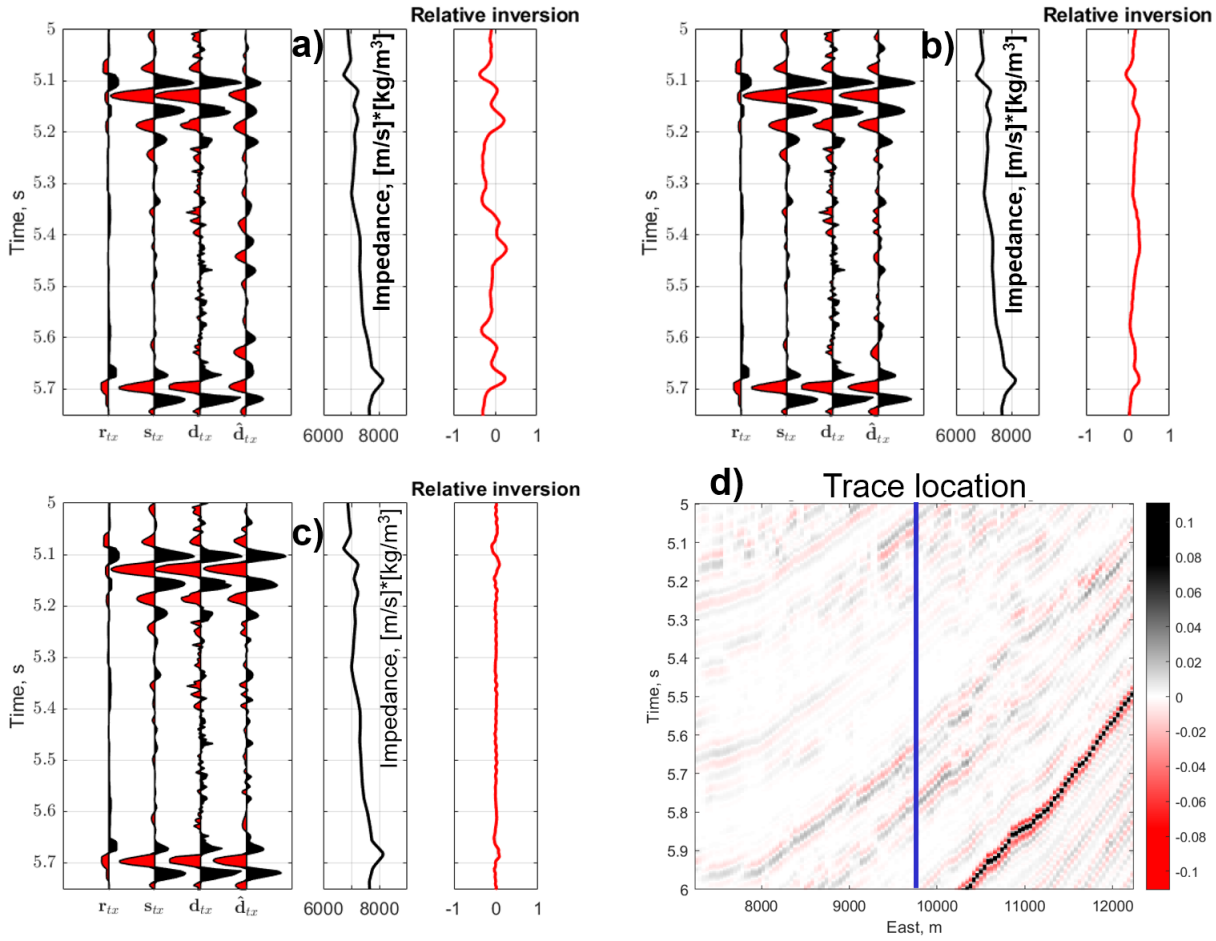

Figure 5: Comparison between relative inversion configurations for trace 55: a) LVA-based inversion; b) constant geometric anisotropy-based inversion; c) regularized inversion; d) seismic record with trace location.

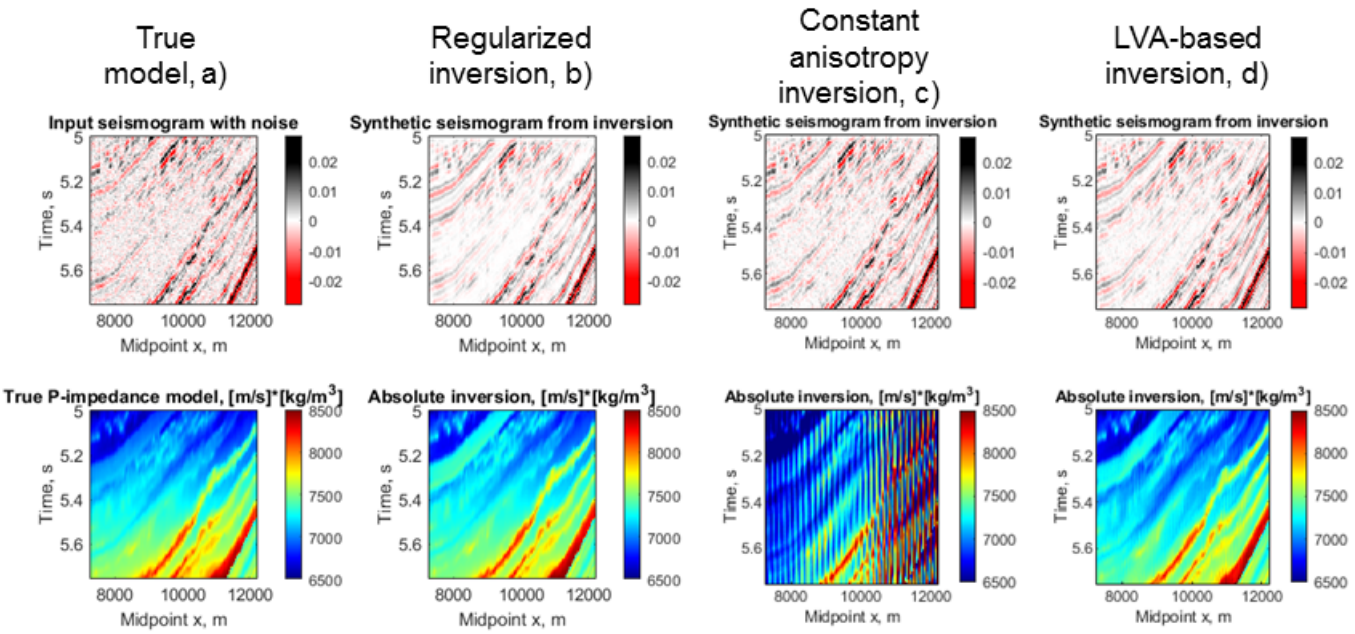

Figure 6: Comparison between absolute inversion configurations. Top row represents seismograms whereas the bottom is P-impedance: a) True model; b) regularized inversion; c) constant geometric anisotropy-based inversion; d) LVA-based inversion.

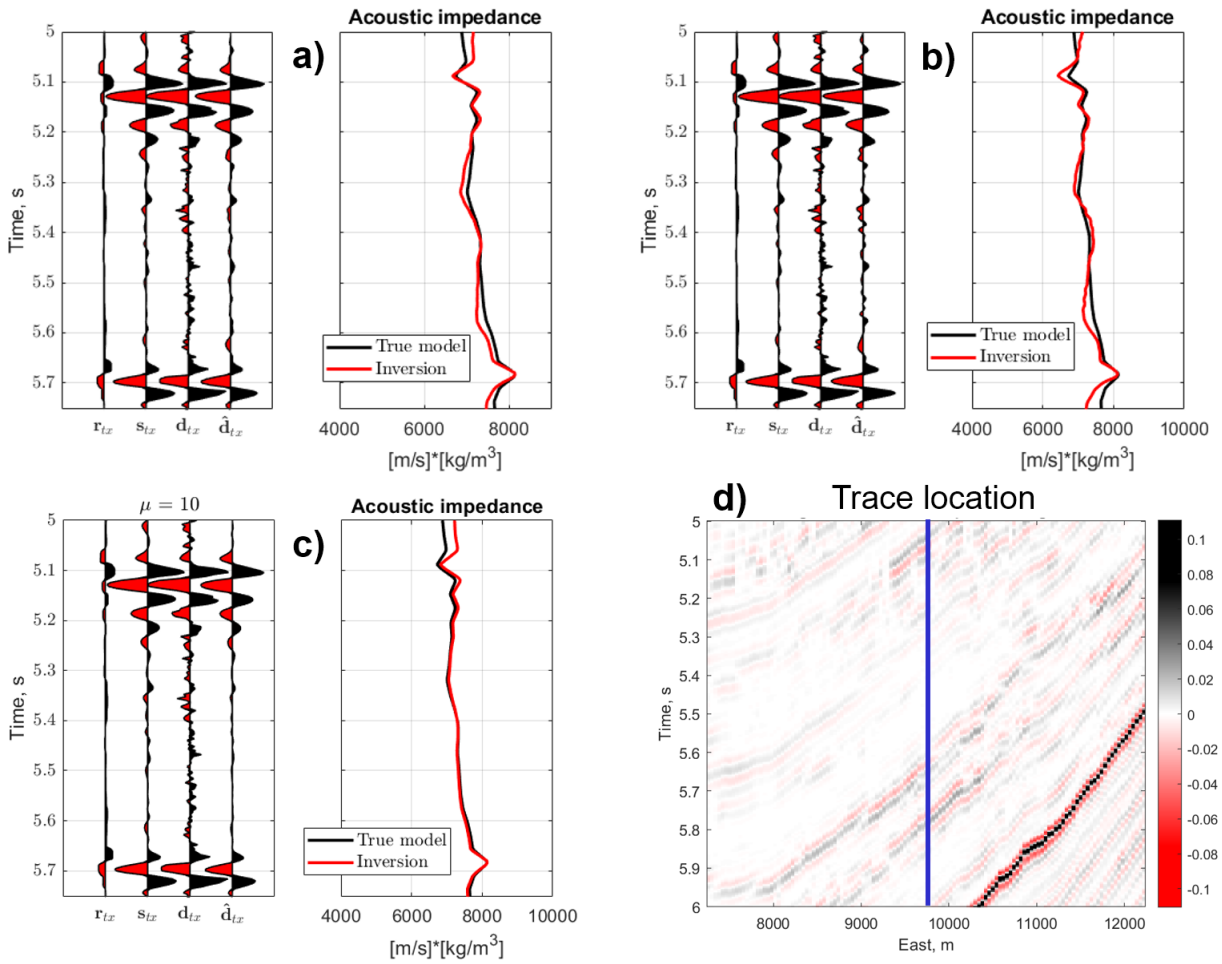

Figure 7: Comparison between absolute inversion configurations for trace 55: a) LVA-based inversion; b) constant geometric anisotropy-based inversion; c) regularized inversion; d) seismic record with trace location.